TELKOMNIKA Indonesian Journal of Electrical Engineering
Vol. 12, No. 8, August 2014, pp. 6036 ~ 6046
DOI: 10.11591/telkomnika.v12i8.5191

Nonuniform Defect Detection of Cell Phone TFT-LCD Display

Jahangir Alam S.M.*, Hu Guoqing
Department of Mechanical & Electrical Engineering, Xiamen University,
Room 228, Science Building, 361005, Siming District, Xiamen, Fujian, China, telp/fax: +86-592-2186393
*Corresponding author, e-mail: jahangir_uits@yahoo.com

Abstract

Uneven and Nonuniformity (Mura) of Thin Film Transistor Liquid Crystal Display (TFT-LCD) is a major problem of cell phone display. The different types of uneven and nonuniformity are decreased the performance of TFT-LCD. To economize and increase its performance, it is necessary to detect these kinds of defects. The cause of these types of noisy defects can be stimulated by the material of TFT, intensity of back light, total internal reflection, mirror form of others materials, internal light, and external light. The energy loss and gain in LCD display is another issue to make these uneven and nonuniformity. The objective of this study is to investigate and detect the defects of cell phone display considering some parameters with image analysis. The back side and the front side of the defects have been observed to find the uniqueness of that defects and its model.

Keywords*: uneven and nonuniformity, defect detection, deviation, energy*

1. Introduction

Now a day, the use of TFT-LCD is very popular. The cell phone display is one of the wide parts of TFT-LCD display. If the performances of mobile phone displays are not higher then it will not be economized. To stimulate the cell phone TFT-LCD display market and attract the customer, it is necessary to produce the non defect TFT-LCD display. To produce the good quality and higher performance TFT-LCD, it is needed to detect the defects such as Mura or uneven defects or nonuniformity. Thus very small scale uneven and nonuniformity can be detected by using Fast Fourier Transform (FFT). The FFT can detect different types of uneven and nonuniformity on cell phone TFT-LCD display. The small sizes of nonuniformity, uneven impact of color, light intensities and energy dissipate, reflected noise are defect on cell phone TFT-LCD display. There are two camera systems that can detect the all types of uneven and nonuniformity which detect by using FFT after that it differentiate the quality of the TFT-LCD display. The characteristics size of non-informal defects and uneven impact can be measured. Then it can be defined the model of the detected defects. Currently, there are many defects detection algorithms has been established [1-8] for TFT-LCD such as Wavelet Transform [1, 2] and level-set method [3]. It is noted that the regression diagnostics algorithm [4] and using adaptive threshold algorithm to detect defect in TFT-LCD are proposed [5, 6] to detect the defects. It has been developed the Minimum Error Thresholding Algorithm by J. Kittler [7].

Image segmentation, threshoulding, FFT analysis, angle adjustment, energy performance analysis are helped to detect the uneven and nonuniformity on TFT-LCD. For high performance and better efficiency, it needs to inspect the image segmentation with its properly window resolution and sizes. It is necessary to distinguish the defect and non defect images then it must be segmented the uneven and/or nonuniformity to detect the defects. These segmented images can be produced by FFT analyzing [9]. Finally all kinds of characteristics can be determined from the model. After successfully defect detection on TFT-LCD, it differentiates the performance of the production.

2. Research Method

High resolution Allied GIGE 4900 and Keyence high speed H200C model cameras have been used to take picture in Figure 1, inspect, and observe the uneven and nonuniformity

Received November 22, 2013; Revised April 3, 2014; Accepted April 20, 2014

on TFT-LCD. To inspection of uneven and nouniformity on mobile phone TFT-LCD, it has been used these two cameras which can capture high resolution images. Two camera has been used for distinguished the differences. To check defects on TFT-LCD, it has been used back light which can controlled by ARM systems. The back light makes the intensity of back side of the TFT-LCD. In the front up side, it inspects the uneven and nonuniformity or any defects.

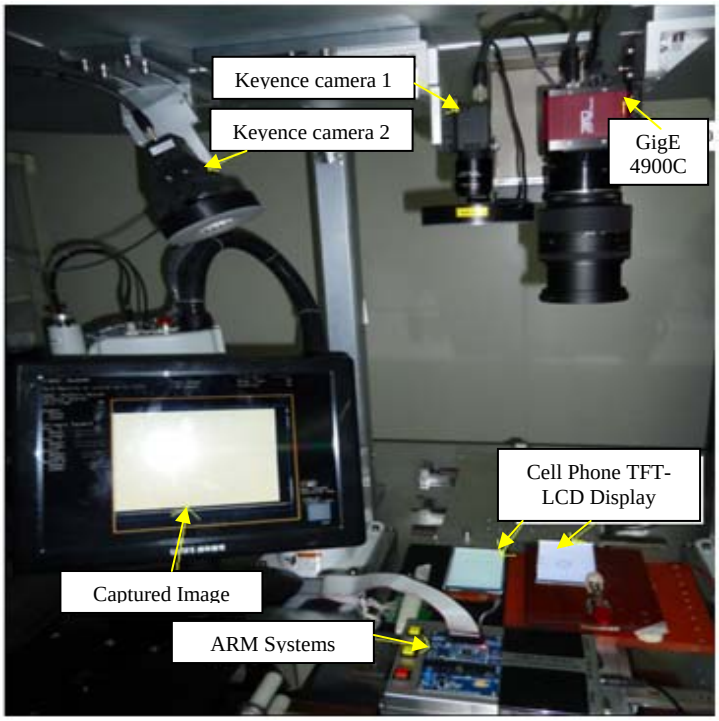

Figure 1. Uneven and Nonuniformity Inspection Equipments

3. Theoretical Analysis

3.1. Fast Fourier Transform

The frequency transform of the Fast Fourier Transform is the most important for frequency responses of any signal [10]. The FFT analysis can detect the uneven and nonuniformity on TFT-LCD which can faster and save the time [1]. To economize and to produce a large amount of product by this method is more efficient and in the robotic vision, it is necessary to detect the defects more vastly. The defects characteristics, position, depth of defect, model of defects, sizes of variations, and back to front sides' inspection, it is necessary to introduce the 3D FFT. The FFT can be modified into 3D FFT to detect the defect as:

$$F(a,b,c) = \frac{1}{NMP}\sum_{x=0}^{N-1}\sum_{y=0}^{M-1}\sum_{z=0}^{P-1} f(x,y,z)e^{-2\pi i\left(\frac{xa}{N}+\frac{yb}{M}+\frac{zc}{P}\right)} \quad (1)$$

Where, $f(x,y,z)$ is the gray level of the world coordinates X,Y,Z of 3D image signal in the Equation (1). Here a,b,c are the coordinates in frequency domain and M, N, P are the size of image axis, respectively. The real images are in the time domain which can be translated into frequency response [9]. Then if there is any defect the frequency response can show the uneven and nonuniformity on the responses by solving the following equation as:

$$S(a,b,c) = 300 \times e^{-(a+b+c)},\ for\ 1 \le a,b,c \le 9 \quad (2)$$

If *a, b* and *c* are small, the value $S(a,b,c)$ is larger. The small *a, b, c* means low frequency region. So, the more low frequency value is multiplied by the larger value [9].

Through this process, the more low frequency component is to put a high proportion and for this purpose the Equation (2) can be rearranged as follows:

$$T(a,b,c) = F(a+1, b+1, c+1) \times S(a,b,c), \quad for \quad 1 \le a,b,c \le 9 \tag{3}$$

$$R(a,b,c) = F(a+1, 129-b, c+1) \times S(a,b,c), \quad for \quad 1 \le a,b,c \le 9 \tag{4}$$

$$U = \frac{1}{162}\sum_{a=1}^{9}\left(\sum_{b=1}^{9}\sum_{c=1}^{9}|T(a,b,c)| + \sum_{b=1}^{9}\sum_{c=1}^{9}|R(a,b,c)|\right) \tag{5}$$

The value U is obtained from Equation (5). If this value larger than specific value G, it is determined that the segmented image has defect. In the opposite case, the segmented image does not have defect. The lower frequency component of segmented image which has defect is larger than that of segmented image which has not defect. The specific value G is defined as follow as:

$$G = \sqrt{\epsilon \times m \times W} \tag{6}$$

Where, $\epsilon = 0.01$, m is gray level mean of the segmented image and W is window size and it is assumed that $W = 128$. The constant value ϵ is obtained experimentally by using Equation (6).

3.2. 3D Discrete Cosine Transform

The 3D Discrete Cosine Transform (DCT) straightforwardly described the 3D measurements from discrete responses [9]. The uneven and nonuniformity also unified by 2D image plane and rest of the dimension can help to detect for characteristics of defects model and source of defects, depth of defects. Thus here the 3D DCT can be defined as follows:

$$X_{k1,k2,k3} = \sum_{n_1=0}^{N_1-1}\left\{\sum_{n_2=0}^{N_2-1}\left(\sum_{n_3=0}^{N_3-3} x_{n1,n2,n3}\, cos\left[\frac{\pi}{N_3}\left(n_3+\frac{1}{2}\right)k_3\right]\right) cos\left[\frac{\pi}{N_2}(n_2 + \frac{1}{2})k_2\right]\right\} cos\left[\frac{\pi}{N_1}\left(n_1+\frac{1}{2}\right)k_1\right]$$

$$\text{i.e. } X_{k1,k2,k3} = \sum_{n_1=0}^{N_1-1}\sum_{n_2=0}^{N_2-1}\sum_{n_3=0}^{N_3-3} x_{n1,n2,n3}\, cos\left[\frac{\pi}{N_1}\left(n_1+\frac{1}{2}\right)k_1\right] cos\left[\frac{\pi}{N_2}(n_2 + \tfrac{1}{2})k_2\right] cos\left[\frac{\pi}{N_3}\left(n_3+\tfrac{1}{2}\right)k_3\right] \tag{7}$$

Here, N_1, N_2, N_3 are 3D DCT length of the axis; n_1, n_2, n_3 is the step from left to right side and front to back or back to front responses which is increased the frequency by 1/2 cycle in the Equation (7). The value of k_1, k_2, k_3 are the scalar factor; $x_{n1,n2,n3}$ is the amplitude scaling of the DCT [1]. The angle of cosine can indicate the angle of defects by using different angle and different position of the cameras shown in Figure 1. It can be increased the efficiency to detect the uneven and nonuniformity of cell phone TFT-LCD display.

The Modified DCT (MDCT) as the lapped transformed is compared to Fourier-related transforms [11] with Equation (7). Usually it has a half of many outputs as inputs. It can be defined as a linear function as, $F: \boldsymbol{R}^{2N} \rightarrow \boldsymbol{R}^{N}$; where $\boldsymbol{R}$ is real number sets. The *2N* real numbers $X_0, \ldots, X_{2N-1}$ can be transformed into the *N* real numbers $X_0, \ldots, X_{N-1}$ according to the formula as:

$$X_k = \sum_{n=0}^{2N-1} x_n cos\left[\frac{\pi}{N}\left(n+\frac{1}{2}+\frac{N}{2}\right)\left(k+\frac{1}{2}\right)\right] \tag{8}$$

The inverse MDCT is known as the IMDCT and this technique is known as time-domain aliasing cancellation (TDAC). The IMDCT transforms *N* real numbers $X_0, \ldots, X_{N-1}$into *2N* real numbers $Y_0, \ldots, Y_{2N-1}$ according to the formula from above Equation (8) can be transformed into IMDCT as:

$$y_n = \frac{1}{N}\sum_{k=0}^{N-1} X_k \cos\left[\frac{\pi}{N}\left(n+\frac{1}{2}+\frac{N}{2}\right)\left(k+\frac{1}{2}\right)\right] \quad (9)$$

In the case of a windowed MDCT with the usual window normalization, the normalization coefficient in front of the IMDCT should be multiplied by 2 (i.e., becoming 2/N). It can be noted for 3D DCT as 2/3. The window has considered for image processing as the IMDCT window and the image signal has been processed as a DCT signal processing [12].

3.2. Nonuniform Discrete Fourier Transform

3D Nonuniform Discrete Fourier Transform (NDFT) [11] of a sequence $x[n_1, n_2, n_3]$ of size $N_1 \times N_2 \times N_3$ is:

$$\hat{X}(Z_{1k}, Z_{2k}, Z_{3k}) = \sum_{n_1=0}^{N_1-1}\sum_{n_2=0}^{N_2-1}\sum_{n_3=0}^{N_3-1} x[n_1, n_2, n_3] Z_{1k}^{-n_1} Z_{2k}^{-n_2} Z_{3k}^{-n_3} \quad (10)$$

Where, $k = 0,1,\ldots,N_1N_2N_3$,$\hat{X}(Z_{1k}, Z_{2k}, Z_{3k})$is the 3D z-transform of$x[n_1, n_2, n_3]$, and (Z_{1k}, Z_{2k}, Z_{3k}) are arbitrarily distinct $N_1N_2N_3$ points in the 4D (Z_1, Z_2, Z_3) space. The above equation (10) can be expressed as the vector form as:

$$\hat{X} = \boldsymbol{D}X \quad (11)$$

Where, the matrix $\boldsymbol{D}$ is also depends only on the choice of those sampling points. However, even if those sampling points are distinct, $\boldsymbol{D}$ could still be singular. No rules for determining whether the matrix is nonsingular or not have been found. Therefore, for all implementation of 3D NDFT, it is needed to just check $\det(\mathbf{D})$ for a specific set of sampling points. This 3D NDFT is helpful to detect for discrete uneven and nonuniformity.

4. Uneven and Nonuniform Detection Process

Size of image is 4872×3276 in Figure 2. The image has been segmented to detect the defects and it performance. The image segmentation important for efficient inspection, each segmented image is overlapped nearby segmented image at least 2 pixels in the horizontal and vertical direction [13]. If segmented image is not overlapped other segmented image, performance of the proposed algorithm tries to defect inspection for each segmented image. The Figure 3 shows the order of inspection of segmented image.

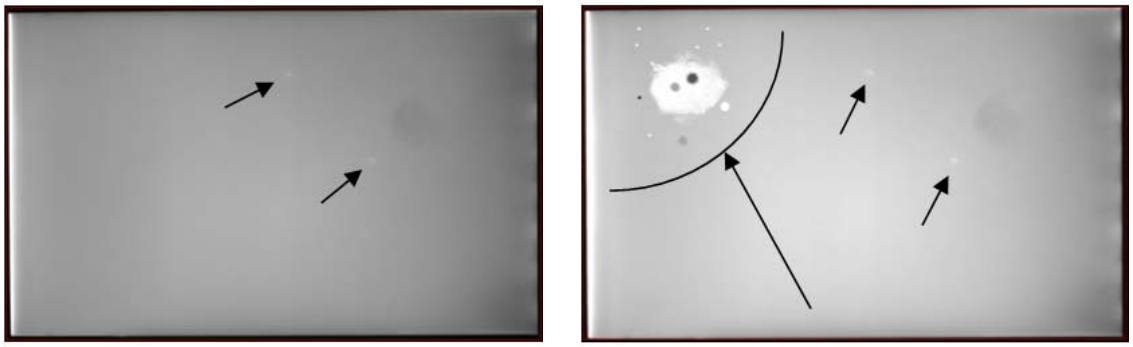

(a) (b)

Figure 2. Uneven and Nonuniform Defects (a) white (b) different types of defects

And then, perform 3D FFT to each segmented image and calculate compactness that is mean of low frequency region. In order to calculate compactness, it has to define low frequency region. The low frequency region is defined as 9-by-9 upper left side except first row and first column and 9-by-9 lower left side except first column. On the cell phone TFT-LCD display panel it can be located there different types of defects or uneven and nonuniformity in Figure 2. To analyze the image here it has been considered the Figure 2(a) that have two defects which are

white points (white unevenn and nonuniformity). After FFT processing, it can look in view of 3D plane in Figure 3. The two peaks value in the Figure 3(a) shows the 3D model of the uneven and nonuniformity on the surface which has been indicated by arrow which is notable. In the Figure 3(b), there are hidden layers representation of uneven and nonuniformity.

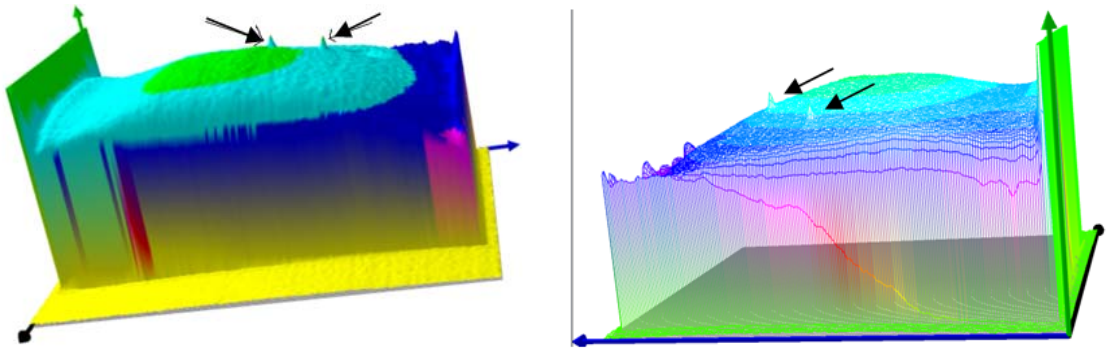

(a) (b)

Figure 3. Uneven and Nonuniformity Check by 3D Contours and Hidden Layers Analysis

5. Results and Discussions

The performance of defect detection of the uneven and nonuniformity have been calculated by different methods. About 100 cell phone TFT-LCD displays were checked as a sample to detect uneven and nonuniformity by using proposed algorithm. The statistics also defined to detect the defect such as Mura or uneven and nonuniformity [12]. The statistical results are inspected by comparing in the defected and non-defected image or cell phone TFT-LCD panel. The defect can be indentified by observing the mean and deviation statistics of the display panel. The mean, variance, and deviation were observed on the display panel in the different positions of the ROI. If there is any defect exist on ROI of TFT-LCD then the mean and variance value is higher than non defect ROI. Mean and deviation can find by following equation:

$$\sigma = \sqrt{\frac{1}{N}\sum_{i=1}^{N}(x_i - \mu)^2}, \; where \quad \mu = \frac{1}{N}\sum_{i=1}^{N} x_i \tag{12}$$

Where, σ is the standard deviation, μ is the mean, x_i is sample space on ROI and N is the number of sample value on ROI. Thus the defects on the cell phone TFT-LCD display can be defined as:

$$f(x,y) = \begin{cases} \text{Defect} & ; \sigma, \mu \text{ much greater than no defect ROI} \\ \text{No defect} & ; \sigma, \mu \text{ much less than defected ROI} \end{cases} \tag{13}$$

Where, x, y is the image plane. The captured image has been segmented for preparing the ROI and checks the box spaces. The filtering process is helpful for eliminating the noise and more concisely. For better analysis and getting better result this process is important to finish the statistical process by using Equation (13). The all processed has been expressed in the following proposed algorithm in Figure 4.

The mean and deviation has been compared by intensity measurement [6]. On cell phone TFT-LCD display, there are some sample space has been created on cell phone TFT-LCD image panel by 'Halcon' software in Figure 5(a). The sample space has been indicated by red square box. The sizes of the square boxes are same. There are two square boxes are indicated by arrow which has an uneven and nonuniformity vastly i.e. there are defected ROI which has been shown as a magnified image in Figure 5(b).

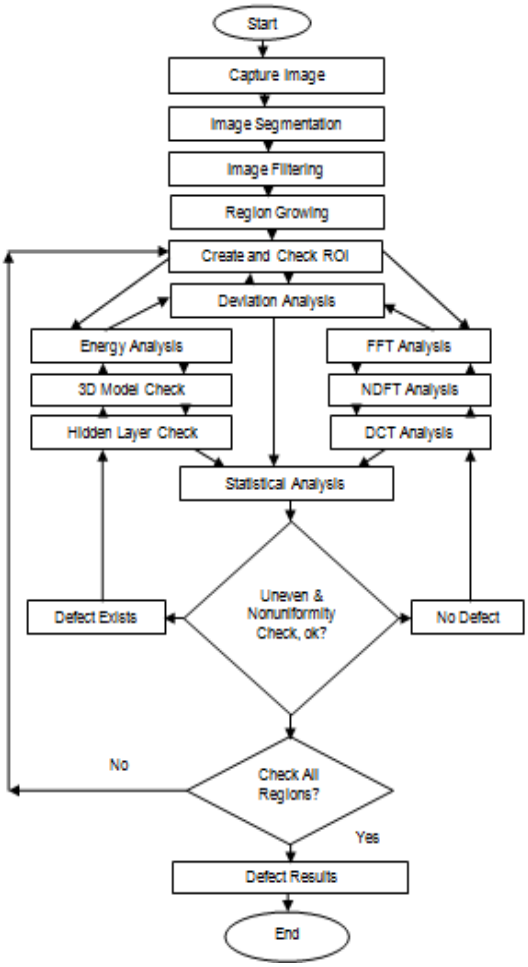

Figure 4. Uneven and Nonuniformity Detection Algorithm

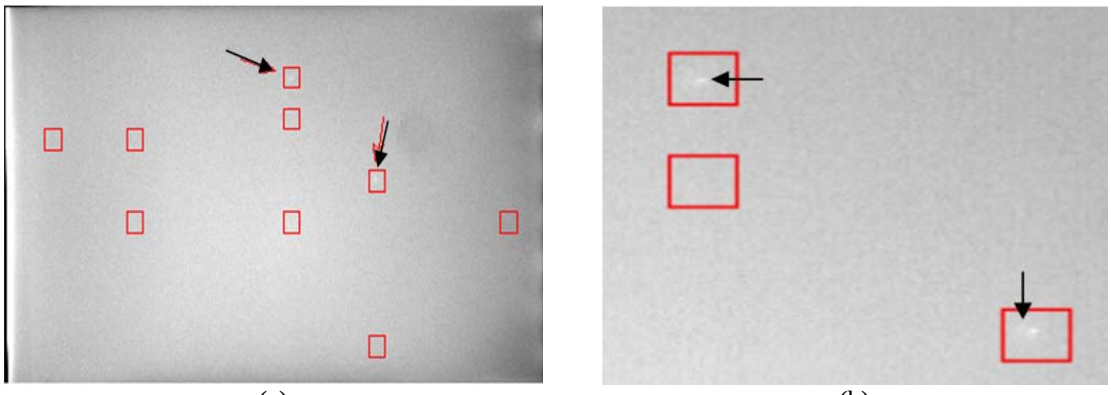

(a) (b)

Figure 5. Intensity Compare on the Cell Phone TFT-LCD Display Panel (a) original, (b) magnifying

The image has been analyzed by 'Halcon' and checked the statistical results as shown in Table 1. The arrow indicated two red squared boxes that have an uneven and nonuniformity and their deviation is higher than other red squared box. The other red squared box on ROI has no defects. The defected two ROI deviations are 6.24 and 6.27.

Table 1. Mean and Deviation on the Cell Phone TFT-LCD Display Panel

	ROI1	ROI2	ROI3	ROI4	ROI5	ROI6	ROI7	ROI8	ROI9
Mean	196.80	201.03	204.33	207.22	206.30	160.17	209.14	223.98	196.76
Deviation	3.86	6.24	4.15	4.17	6.27	4.49	4.01	4.22	4.49

The Figure 6 shows the region growing simulation results for uneven situation and nonuniform defect detection. The captured image has been processed into median images as a mirror image. In the median image, there is generated a circle in tolerance which can accept the ROI pixel value. The median image divides into segment for region growing [14]. The 'regiongrowing' method is used to find the defects. The tolerance of the 'regiongrowing' is around 2 pixels to 3 pixels for this detection. In the 2 pixel to 3 pixel tolerance, the indicated uneven and nonuniformity can be detected by using 'Halcon' software in Figure 6(a) and Figure 6(b) shows that the indicated circle of defects are smaller tolerance. Out of this tolerance all defects also can be detected by this method.

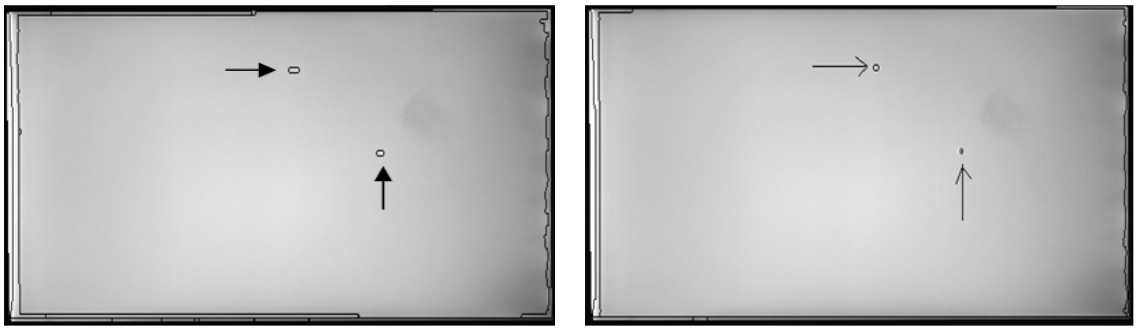

(a) (b)

Figure 6. Defect Detection by Region Growing at Tolerance (a) 3 level, (b) 2 level

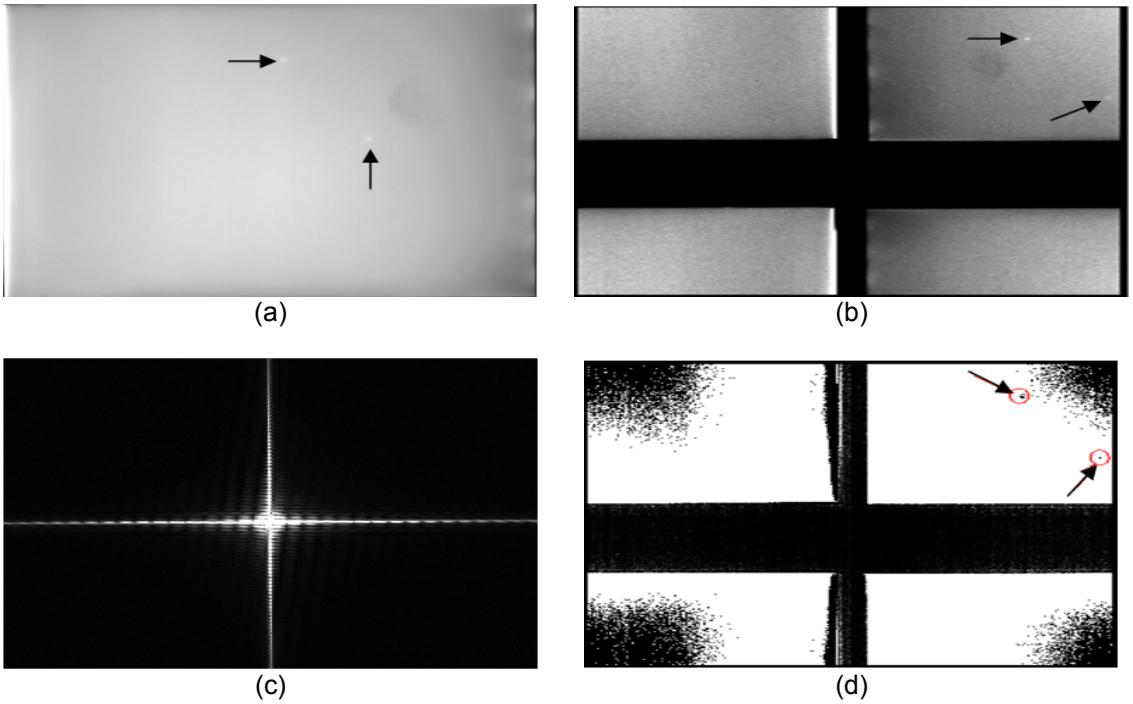

(a) (b)

(c) (d)

Figure 7. FFT Processing of Defected TFT-LCD Display (a) filtered image, (b) convolution FFT, (c) image FFT, (d) correlation FFT

The Figure 8 shows there is no defect of the TFT-LCD display panel. Here it is processed the image with similar way by 'Halcon'. Since in this cell phone TFT-LCD display panel has no defects or uneven situation and nonuniformity in Figure 8, therefore, there are no uneven and nonuniformity events on the panel. The comparison of Figure 7 and Figure 8 shows that whether there is any defect or not. By using equation (11), it also has been determined that the uneven and nonuniformity is absent.

Depth of defects can be found from focus that is called Depth From Focus (DFF) [10]. This is a method that enables the reconstruction of 3D surface information of several images taken at different focus distances between camera and the defects. With depth from focus, it can be reconstructed the surface of a 3D defect based on the knowledge that defect region has different distances to the camera and the camera has a limited depth of field in Figure 3. Depending on the distance and the focus, the defects region are displayed more or less sharply in the image, i.e., only those pixels within the correct distance to the camera are focused. Taking images with various points on the defects to measure the distances, each defect point on the defect region can be displayed sharply in at least one pixel of an image. Such a sequence of images is called "focus stack" [14]. By determining in which image an object point is in focus, i.e., sharply imaged, the distance of each defect point on the defect region to the camera can be calculated [14]. This principle is displayed in Figure 9.

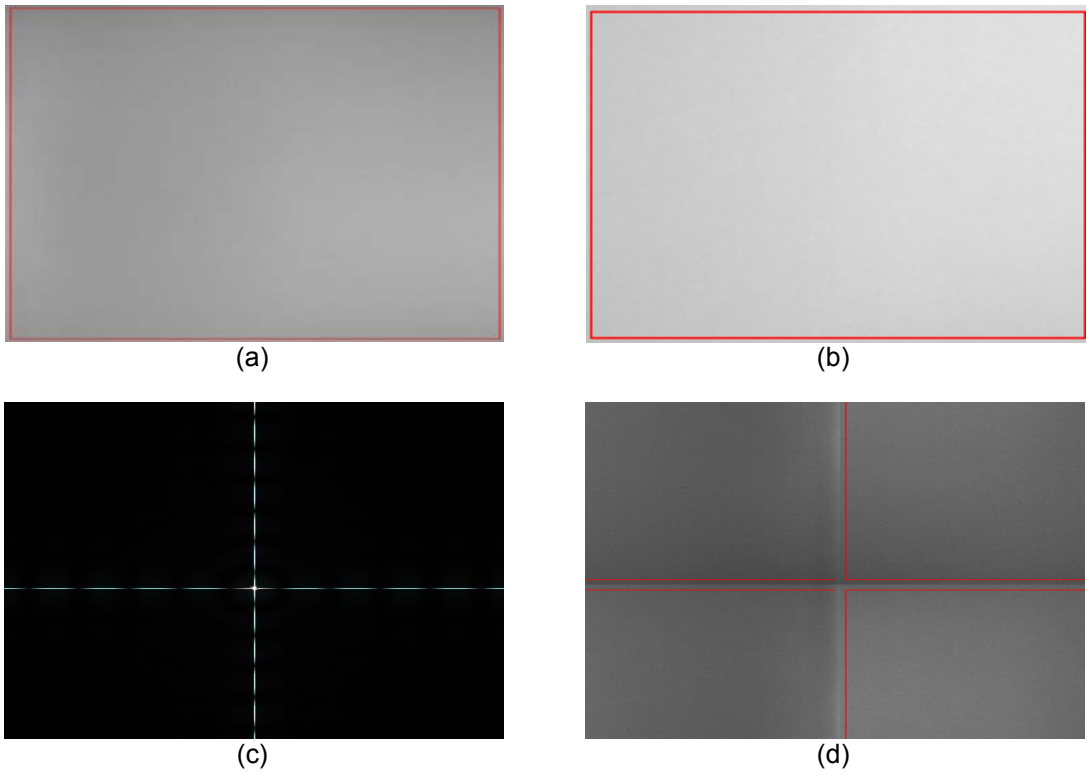

Figure 8. FFT Processing of Non-defected TFT-LCD Display (a) filtered image, (b) convolution FFT, (c) image FFT, (d) correlation FFT

If the maximum focus pixel length is Δf_{max} and the length of depth in hidden layer is Δh_{max}, then the total 3D defected pixel length is $L_D = \Delta f_{max} + \Delta h_{max}$ along with Z-axis, in the image plane if the defect length is Δx to X-axis and the Δy to the Y-axis then the defect depth in pixel can be defined as:

$$D_p = \int_{-x}^{x} \int_{-y}^{y} \int_{-z}^{z} (L_D \, \Delta x \, \Delta y \,) \, dx \, dy \, dz \quad (14)$$

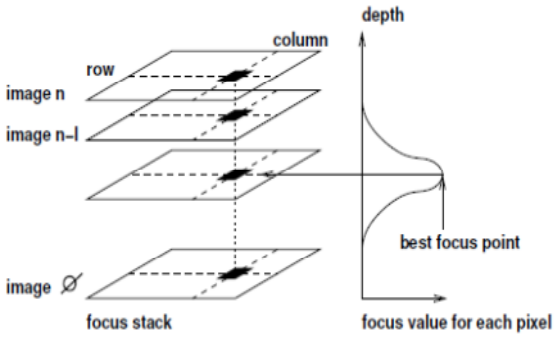

Figure 9. DFF on 3D Plane of Cell Phone TFT-LCD Display

The Figure 10 shows the back side of the defects. The peak value of the back side and the front side are not same. The intensity of back side and front side are not same which can be compared with Figure 5.

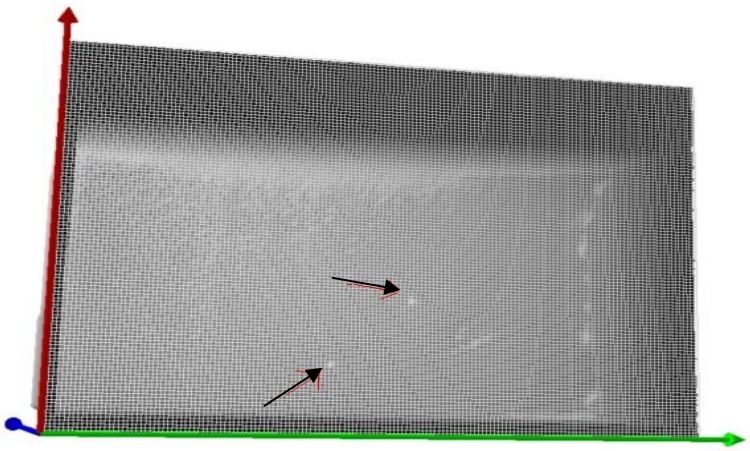

Figure 10. 3D Checking from the View of Back Side of Defects

The defects are usually non linear thus the non linear defects in Figure 3(b) can be expressed as the autoregressive model as:

$$X_t = a + \sum_{j=0}^{u}(\alpha_i X_{t-j})h_j + \in_t \quad (15)$$

Where, α_i is the coefficients parameters, a is the constant value, h_j is the hiden layers parameters and $\in_t$ is the white noise of the linear defects model [13, 15]. The back shift operator can stimulate the model by β^j and then the Equation (15) can be written as:

$$X_t = a + \sum_{j=0}^{u}(\alpha_i \beta^j X_{t-j})h_j + \in_t \quad (16)$$

The polynomial representation of the defect model can be expressed as:

$$\emptyset(\beta)h_j X_t = a + \in_t \quad (17)$$

The back shift operator and the hidden layer parameters of the non linear equation can be shocked of the defects model. The source of the uneven and the nonuniformity and the depth of defects can be finalized by the following model.

$$X_t = \frac{1}{\emptyset(\beta)h_j}(a + \in_t) \quad (18)$$

Finally the power spectral density of the model is correlated and the variance is related to the consumption of the defects. Thus it can be expressed as:

$$M(f) = \frac{\sigma_z^2}{\left|1-\sum_{j=0}^{u}\alpha_j e^{-2\pi ijf}\right|^2} \quad (19)$$

$$Or,\ M(f) = \frac{\sigma_z^2}{1+\alpha_1^2+\alpha_2^2-2\alpha_1(1-\alpha_2)cos(2\pi f)-4\alpha_2 cos(4\pi f)} \quad (20)$$

Where, σ_z^2 is the variance, f is the frequency response, j is the index term. The energy calculation of the uneven and nonuniformity is shown in Table 2. It is noted that the energy level of the defects are higher than the non-defected ROI in Figure 5. There are two highest two peak energy level for the above non-linear defects model as 0.1067 and 0.1017 on the defected region ROI2 and ROI5 in Figure 5.

Table 2. Energy Dissipate by the Defects

	ROI1	ROI2	ROI3	ROI4	ROI5	ROI6	ROI7	ROI8	ROI9
Energy (mV)	0.0343	0.1067	0.0486	0.0487	0.1017	0.0795	0.0869	0.0653	0.0301

6. Conclusion

This work represents uneven and nonuniformity (Mura) detection algorithm of cell phone TFT-LCD display by using different techniques such as 3D FFT, 3D DCT, 3D MDCT, and NDCT. It is proposed a novel detection algorithm for the cell phone TFT-LCD display consisting image segmentation, filtering, and 3D characteristics. Image segmentation and filtering are the efficient process to complete this work. In the 3D FFT processing it can able to determine the low frequency information after that it compute the depth and characteristics of defected model easily. This information can be important for uneven and nonuniformity detection on mobile phone TFT-LCD display for higher performance and better efficiency.

Acknowledgements

Warm expression and sincere thanks to China United Tech. Co. Ltd., Shenzhen, China especially to Mr. David Huang, Li Ming, Ou Ji Heng and Guo Bo for their support to accomplish the experiment.

References

[1] Chen SL, Chou ST. TFT-LCD Mura defect detection using wavelet and cosine transforms. *J. Adv. Mech. Des. System*. 2008; 2: 441-453.
[2] Song TC, Choi DH, Park KH. Wavelet based image enhancement for defect detection in thin film transistor liquid crystal panel. *Jpn. J. Appl. Physics.* 2006; 45(6A): 5016–5072.
[3] Xin B, Chungang Z, Han D. A new mura defect inspection way for tft-lcd using level set method. *IEEE Signal Process. Letter.* 2009; 16(4): 311–314.
[4] Fan SK, Chuang YC. Automatic detection of Mura defect in TFT-LCD based on regression diagnostics. *Pattern Recognition Letters.* 2010; 31: 2397-2404.
[5] Noh CH, Lee SL, Kim DH, Chung CW, Kim SH. An effective and efficient defect inspection system for TFT-LCD polarised films using adaptive thresholds and shape-based image analyses. *International Journal of Production Research.* 2010; 48(17): 5115-5135.
[6] Kim SY, Song YC, Jung CD, Park KH. Effective defect detection in Thin Film Transistor Liquid Crystal Display images using adaptive multi-level defect detection and probability density function. *Optical Review.* 2011; 18(2): 191-196.
[7] Kittler J, Illingworth J. Minimum error thresholding. *Pattern Recognition.* 1986; 19: 41-47.
[8] Yun JP, Choi S, Seo B, Kim SW, Real-time vision-based defect inspection for high-speed steel products. *Optical Engineering.* 2008; 47(7).

[9] Nam KK, Jong SL, PooGyeon Park. Mura Region Detection by Using 2D FFT with Exponential Kernel for Black Resin-Coated Steel. *Intl Journal of Info & Electronics Engg*. 2012; 2(6): 932-935.
[10] Zhiliang Wang, Jian Gao, Chuanxia Jian, Yu Cen, Xin Chen. OLED Defect Inspection System Development through Independent Component Analysis. *TELKOMNIKA Indonesian Journal of Electrical Engineering*. 2012; 10(8): 2309-2319.
[11] Marvasti F. Nonuniform Sampling: Theory and Practice. Plenum Publishers Co. 2001: 325-360.
[12] Liang-Chia Chen, Chia-Cheng Kuo. Automatic TFT-LCD Mura defect inspection using discrete cosine transform-based background filtering and 'just noticeable difference' quantification strategies. *Measurement Science and Technology*. 2008; 19: 1-10.
[13] Shu-Kai S Fan, Yu-Chiang Chuang. Automatic detection of Mura defect in TFT-LCD based on regression diagnostics. *Pattern Recognition Letters*. 2010; 31: 2397-2404.
[14] Yuan Jia-Zheng, Li Qing, Sun Bo-xuan. Multi-focus Image Fusion Based on Region Segmentation. *TELKOMNIKA Indonesian Journal of Electrical Engineering*. 2013; 11(11): 6722-6727.
[15] Qiao C, Songhua H, Xiangyang X, Bo Li. Linear Modeling for Spectral Images Based on Truncated Fourier Series. *TELKOMNIKA Indonesian Journal of Electrical Engineering*. 2013; 11(9): 5245-5252.